Journal of Hazardous Materials 162 (2009) 423–429

Contents lists available at ScienceDirect

Journal of Hazardous Materials

journal homepage: www.elsevier.com/locate/jhazmat

# Selective elimination of lead(II) ions by alginate/polyurethane composite foams

Hiroaki Sone, Bunshi Fugetsu*, Shunitz Tanaka

*Laboratory of Environmental Remediation, Graduate School of Environmental Science, Hokkaido University, Sapporo 060-0810, Japan*

ARTICLE INFO

*Article history:*
Received 26 March 2008
Received in revised form 14 May 2008
Accepted 14 May 2008
Available online 24 May 2008

*Keywords:*
Alginate
Carboxyl groups
Polyurethane foams
Ion exchange
Lead(II) ions

ABSTRACT

A new type of adsorbent which is capable of selectively adsorbing lead(II) ions ($Pb^{2+}$) was developed. The adsorbent was generated by reaction of sodium alginate with NB-9000B, a polyisocyanate type of prepolymer of polyurethane. The adsorbent was a hydrophilic and flexible alginate/polyurethane composite foam (ALG/PUCF) with the alginate chemically immobilized in the cell walls of the foam. Acid–base titration was used to quantify the concentration of carboxyl groups, which are present on the alginate molecules of the ALG/PUCF, functioning as the essential sites for binding $Pb^{2+}$. For the optimized ALG/PUCF, the carboxyl was found to be $38.2 \pm 1.2$ μmol/g of dry weight. The capacity for adsorbing $Pb^{2+}$ ions in 1.0 g of dry weight of the optimized ALG/PUCF was found to be $16.0 \pm 2.1$ μmol, indicating that ion exchange was the essential mechanism for adsorbing $Pb^{2+}$ ions. The adsorption capacity was found to be highly sensitive to the pH of the sample solution; lower pH (<3) significantly decreased the adsorption. Competing ions such as $Mg^{2+}$, $Ca^{2+}$, and $Cd^{2+}$ also caused a decrease in selectivity and capacity for $Pb^{2+}$ adsorption, although the effect was less pronounced than the effect of pH. The ALG/PUCF is highly stable, flexible and easy to use. ALG/PUCF is also reusable after regeneration with ethylenediamine-*N*,*N*,*N*′,*N*′-tetraacetic acid, disodium salt (EDTA-2Na). Due to these features, this adsorbent may be highly useful for elimination of $Pb^{2+}$ ions from contaminated water.

© 2008 Elsevier B.V. All rights reserved.

## 1. Introduction

Elimination of lead (Pb) from contaminated environments is important for a number of reasons. Firstly, Pb is toxic to humans via interaction with the sulfhydryl group of proteins, resulting in disruption of the metabolism and biological activities of many proteins [1]. Pb also impairs hemoglobin synthesis and can cause damage particularly to the liver and kidneys, as well as causing neurological disorders [2,3]. Secondly, Pb is toxic to plants. Free lead(II) ions ($Pb^{2+}$) accumulate primarily within the cell walls and intercellular spaces, causing reduction in root growth and loss of apical dominance of plants, even at very low concentrations (for example, at 0.2 μM) [4]. Thirdly, many industrial effluents and/or wastewater discharged from the production processes of lead-acid batteries, paint, oil, and lead-petrol contain a considerable amount of Pb. Leakage of Pb from these effluents and wastewater into groundwater can cause serious groundwater contamination [5]. In some cases, water extracted from soil subjected to lead contamination was found to contain free $Pb^{2+}$ ions as high as 1.0 μM [6].

Elimination of Pb from lead-contaminated environments is therefore a very important task in the field of environmental remediation. For the elimination of Pb, particularly in the form of free $Pb^{2+}$, from the contaminated aqueous solutions (wastewater), physical adsorption onto an inert material is the mostly widely used method. Other methods, such as ion exchange [7], chemical precipitation [8], electrochemical reduction [9], and electro-dialysis [10] were also found to be useful. For physical adsorption, activated carbon is traditionally used as the adsorbent [11–13]. Because of its high porosity, very high surface area and relatively high mechanical strength, activated carbon has a large capacity for the removal of $Pb^{2+}$ ions. However, activated carbon is unable to selectively adsorb $Pb^{2+}$ ions, resulting in an unpredictable lifespan for the adsorbent [14].

In recent years, the use of naturally produced materials, such as waste biomass, as adsorbents for environmental remediation has received great attention. The utilization of waste biomass is of great interest because these materials represent unused resources and in many cases present serious disposal problems. Numerous sources of waste biomass are available and some studies have demonstrated that such materials are capable of selectively adsorbing heavy metal ions [15–18]. Various functional groups such as phosphate, carboxyl, amine and/or amide are involved in the adsorption of the heavy metal ions, which occurs as a result of ion exchange or ion-complex formation.

Alginate, the main component of brown algae (a typical marine biomass), is a polysaccharide biopolymer composed of anionic

* Corresponding author. Tel.: +81 11 706 2272; fax: +81 11 706 2272.
*E-mail address:* hu@ees.hokudai.ac.jp (B. Fugetsu).

0304-3894/$ – see front matter © 2008 Elsevier B.V. All rights reserved.
doi:10.1016/j.jhazmat.2008.05.093

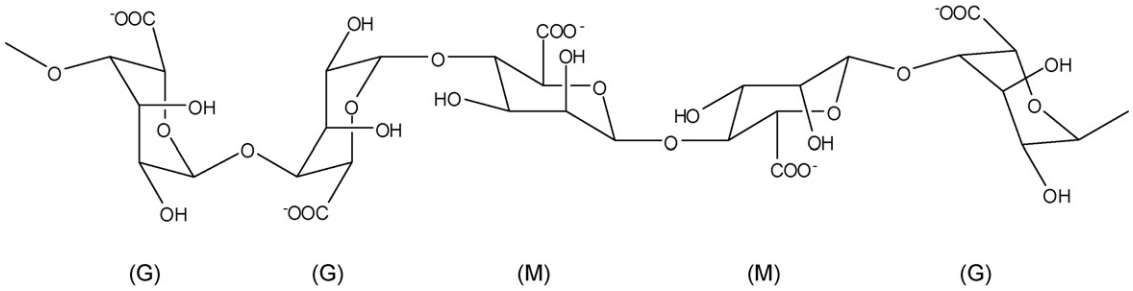


**Scheme 1.** Typical structure of alginate; carboxyl groups are the functioning sites for binding heavy metal ions.

blocks of 1,4 linked α-L-gluronic acid (G) and β-D-mannuronic acid (M); Scheme 1 shows the typical structures. Carboxyl groups are the functioning sites for binding heavy metal ions and the capability of alginate to bind heavy metal ions was investigated in previous studies that showed a higher affinity for $Pb^{2+}$ ions compared to other metals [19]. Alginate is soluble in water. Formation of hydrogels from alginate using divalent cations ($Ca^{2+}$ or $Ba^{2+}$) as the cross-linked ions has long been the standard method for preparing water-insoluble, alginate-based adsorbents. The intrinsic mechanical weakness of the hydrogels, however, has greatly restricted the application of alginate for wastewater treatment. Although alginate can also be blended with other molecules such as cellulose [20] to increase its mechanical strength, developing alginate-based materials of high mechanical strength remains a challenge.

In this study, we focus on polyisocyanate, which is capable of interacting with alginate to give flexible polyurethane foams of high mechanical strength. The polyurethane prepolymer, derived from a poly(oxy C2-4 alkylene) diol and toluene diisocyanate having three isocyanate functionalities, was mixed with an aqueous solution containing sodium alginate to produce hydrophilic, flexible alginate/polyurethane composite foams (ALG/PUCF). The resulting foams showed high capability for adsorbing lead(II) ions from the model water samples, demonstrating their applicability for elimination of $Pb^{2+}$ ions from contaminated water. The ALG/PUCF were reusable by regenerating the foams with ethylenediamine-*N*,*N*,*N*′,*N*′-tetraacetic acid, disodium salt (EDTA-2Na).

## 2. Materials and methods

### 2.1. Materials

Sodium alginate (300–400 cp) was obtained from Wako Pure Chemicals (Osaka, Japan). Polyurethane prepolymers, derived from a poly(oxy C2-4 alkylene) diol and toluene diisocyanate (TDI) having three isocyanate functionalities, were provided by INOAC Corporation (Nagoya, Japan). The prepolymer is called NB-9000B and its chemical structure is depicted in Scheme 2. Triblock copolymer poly(ethylene oxide)-*block*-poly(propylene oxide)-*block*-poly(ethylene oxide) ($EO_6PO_{36}EO_6$, trade name Pluronic L-62), which was used as the surfactant for strengthening the cell walls of the flexible foams, was also provided by INOAC Corporation. Inorganic salts, $CaCl_2{\cdot}2H_2O$, $Cd(NO_3)_2$, $MgCl_2{\cdot}6H_2O$, and $Pb(NO_3)_2$, used to prepare the model aqueous samples containing the corresponding metal ions, were obtained from Wako Pure Chemicals. All these materials were used as received.

### 2.2. Synthesis of ALG/PUCF

The ALG/PUCF were obtained by mixing the polyurethane prepolymer NB-9000B with the aqueous sodium alginate (ALG) solution and the triblock copolymer Pluronic L-62. Pluronic L-62 controls the pore size of the ALG/PUCF by formation of the reverse type of micelles. The mixing ratio (w/w/w) for NB-9000B, aqueous sodium alginate solution, and Pluronic L-62 was 100/100/1.

### 2.3. Adsorption experiments

A piece of ALG/PUCF of approximately 0.5 g (dry weight) was immersed in a test tube containing 100 ml of the aqueous solution containing the heavy metal and was then shaken using a vortex shaker. The pH of the aqueous solutions was adjusted with nitric acid and ammonium solution. After the adsorption had equilibrated, the ALG/PUCF adsorbent was removed from solution. The concentration of the remaining metal ions in the solution was analyzed using inductively coupled plasma atomic emission spectrometry (ICP-AES). An ICP-AES-7000 sequential plasma spectrometer (Shimadzu, Kyoto, Japan) was used. The following wavelength lines were used: 393.366 nm (Ca), 226.502 nm (Cd), 228.616 nm (Co), 279.553 nm (Mg), 257.610 nm (Mn), and 220.351 nm (Pb).

### 2.4. Preparation of cross-linked $Ca^{2+}$–alginate hydrogel beads

Alginate-based adsorbents obtained by the conventional method of hydrogel formation with calcium(II) ions ($Ca^{2+}$) as the linkage ions were prepared for comparison to the novel adsorbent developed in this work. An IER-20 encapsulation system (Inotech, Dottikon, Switzerland) was used to prepare the $Ca^{2+}$–ALG hydrogel beads [21]. The ALG solution (1.5%, w/v) was forced into a pulsation chamber using a syringe pump. The aqueous ALG solution was then passed through a precisely drilled sapphire nozzle of diameter 200 μm and was separated into droplets of equal size upon exiting the nozzle. These droplets passed through the electrostatic field between the nozzle and an O-ring electrode, acquiring electrostatic charges on their surfaces. Electrostatic repulsion forces dispersed the droplets as they fell into the aqueous hardening solution containing 100 mmol/l of calcium dichloride. The resulting beads were rinsed thoroughly with deionized water and were then collected using a 100 μm mesh sieve.

## 3. Results and discussion

### 3.1. Structure of the hydrophilic, flexible ALG/PUCF

Fig. 1 shows scanning electron microscope (SEM) images together with a digital photo of the ALG/PUCF. As seen in Fig. 1, like the common flexible polyurethane foams, the ALG/PUCF established in this study consists of three-dimensional agglomerations of gas bubbles, separated from each other by thin sections of the host medium. The thin structures separating the bubble spaces (also referred to as cell walls) are co-polymers of alginate and the polyurethane prepolymer NB-9000B, formed through various reac-

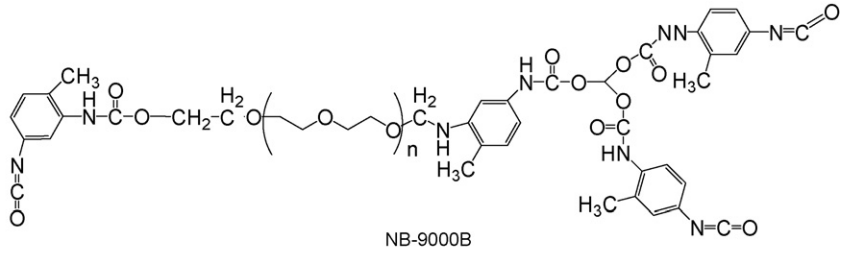


R-NCO + HO-R' → R-NHCOO-R' (a)

R-NCO + $H_2O$ → [R-NHCOOH] → R-$NH_2$ + $CO_2$ (b)

RNCO + R-NHCOO-R' → R-N(CONHR)COO-R' (c)

**Scheme 2.** Structures of the polyurethane prepolymer, NB-9000B, and the reactions involved in the polyurethane foam formation: (a) chain extension reaction, (b) foam formation reaction and (c) cross-linking reaction.

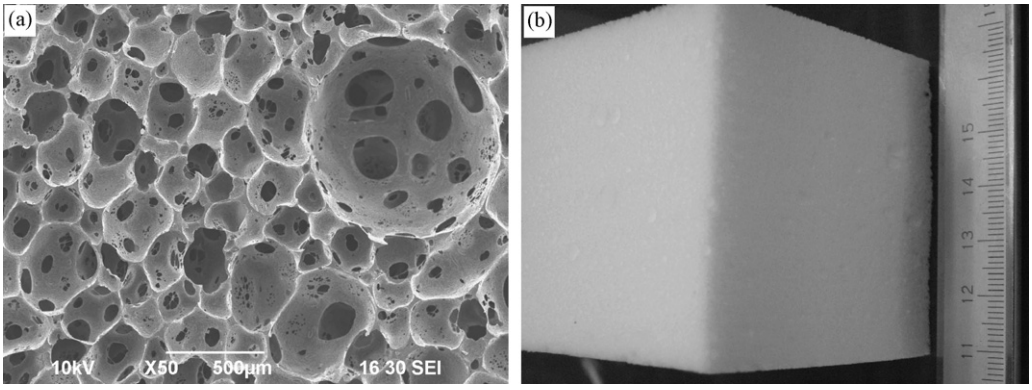


**Fig. 1.** SEM image of the flexible sodium–alginate/polyurethane composite foam (ALG/PUCF) at 50× magnification (a) and a digital photo (b) of the same ALG/PUCF at low resolution.

tions (chain extension reaction, foam formation and cross-linking reaction). Fig. 2 shows FT-IR spectra of the ALG/PUCF together with the spectra for sodium alginate alone. The characteristic band corresponding to isocyanate (–N=C=O) at about 2230 $cm^{-1}$ was not observed, suggesting that the NCO groups have completely reacted. In addition, bands at 3295 $cm^{-1}$ (corresponding to NH), 1724 $cm^{-1}$ (corresponding to free –C=O), and 1530 and 1221 $cm^{-1}$ (corresponding to NH and CN, respectively) were observed, indicating the formation of the urethane–urea bond. Moreover, asymmetric and symmetric stretching vibrations of $COO^-$ (which was the functional group for binding $Pb^{2+}$ ions) at 1598 and 1410 $cm^{-1}$ were observed, indicating that alginate was grafted on the polyurethane prepolymers, NB-9000B. Furthermore, the band corresponding to –OH in the alginate at 3440 $cm^{-1}$ disappeared; suggesting that –OH in the alginate has reacted with NB-9000B. Note that the characteristic absorption for alginate at 946 $cm^{-1}$ (1,4 linkage), 877 $cm^{-1}$ (β-mannuronic residues) and 814 $cm^{-1}$ (α-guluronic residues) were overlapped by the characteristic bands for PUF, making the FT-IR band assignment of the backbone for alginate in ALG/PUCF difficult.

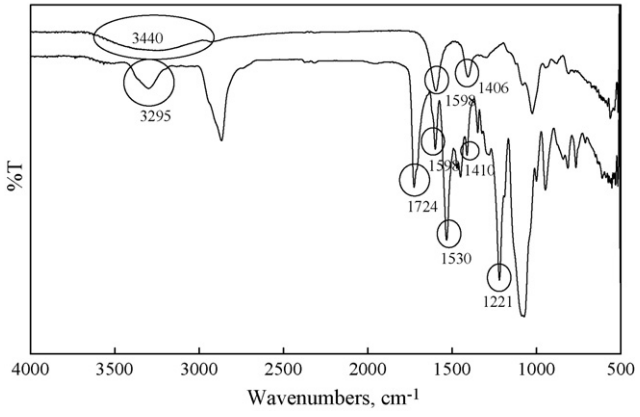


**Fig. 2.** FT-IR spectra of sodium alginate (upper line) and of the ALG/PUCF (lower line).

### 3.2. Quantitative analysis of carboxyl groups in ALG/PUCF using acid–base titration

In order to quantify the carboxyl groups in ALG/PUCF, acid–base automatic titration was carried out using an AUT-501 instrument (TOA Electronics, Tokyo, Japan). A certain amount (0.4–0.6 g) of dry weight of ALG/PUCF was immersed in 0.10 mol/l hydrochloric acid solution to obtain ALG of acidic form. This was then rinsed with deionized water until free HCl was completely removed. This was assayed by adding silver nitrate to the rinsed solution and observing the precipitated product of silver chloride. After conversion to acidic form, the ALG/PUCF was immersed in 25.0 ml of 10.0 mmol/l sodium hydroxide (NaOH); the concentration of the unreacted NaOH was then determined by titration with 10.0 mmol/l hydrochloric acid solution. A typical titration curve is shown in Fig. 3. The ALG/PUCF obtained by using a 1.0% ALG aqueous precursor solution was found to contain 38.2 ± 1.2 μmol carboxyl groups for 1.0 g of the dry weight of ALG/PUCF.

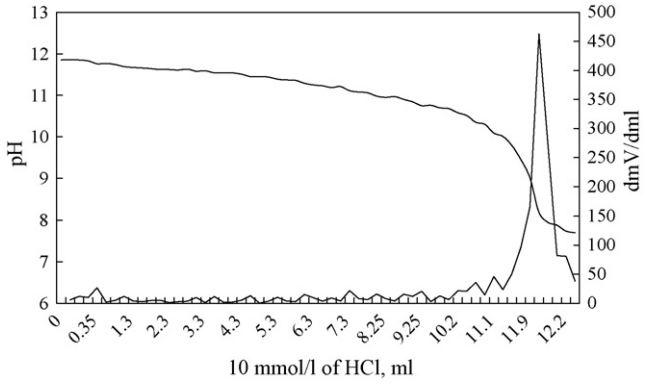


**Fig. 3.** Potentiometric and conductometric back titration of NaOH achieved by stepwise addition of 10.0 mmol/l of HCl.

### 3.3. Effect of contact time and pH on the adsorption of $Pb^{2+}$ ions

Approximately 0.5 g of the dry weight of ALG/PUCF was soaked and shaken in 100.0 ml of an aqueous solution containing 100.0 μmol/l of $Pb^{2+}$ ions. The concentration of $Pb^{2+}$ in this solution was measured using ICP-AES. Fig. 4 shows the change in the concentration of $Pb^{2+}$ as a function of the contact (adsorption) time. Adsorptions with the sole PUF (the reference adsorbent not containing ALG) were also performed under identical experimental conditions. The results are given in Fig. 4 for comparison. As can be seen from Fig. 4, the ALG/PUCF was capable of adsorbing $Pb^{2+}$ ions with the adsorption equilibrium being reached within 15 min. In contrast, the sole PUF led to very little reduction in $Pb^{2+}$ concentration. This comparison of the two adsorption curves shows that alginate (ALG) is the functional site for capturing the $Pb^{2+}$ ions. The capture of $Pb^{2+}$ by ALG/PUCF was quantified by energy dispersive X-ray spectrometry. Fig. 5 shows the experimental data; ALG/PUCF containing Pb was confirmed.

The ability of the ALG/PUCF to adsorb $Pb^{2+}$ was found to depend strongly on the pH of the sample solution. As seen in Fig. 6, the adsorption ability decreased as the pH of the sample solution shifted to the acidic range. The ALG/PUCF has shown almost no ability to adsorb $Pb^{2+}$ ions for the sample having pH 0.98 and very low capacity at pH 2.05. For the samples having pH 3.96 and/or larger, however, the ALG/PUCF performs at nearly maximum capacity, indicating that the adsorption is achieved by the carboxyl moieties

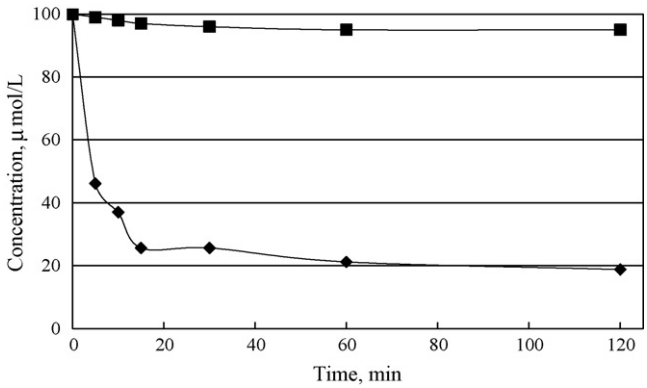


**Fig. 4.** Change in $Pb^{2+}$ concentration as a function of adsorption time using ALG/PUCF (♦). The sample was 100.0 ml aqueous solution containing $Pb^{2+}$ ions at an initial $Pb^{2+}$ concentration of 100.0 μM; pH 4.02; ALG/PUCF = 0.502 g (dry weight). Adsorption experiments were also performed using sole PUF (not containing alginate, ■) as the adsorbent under identical experimental conditions.

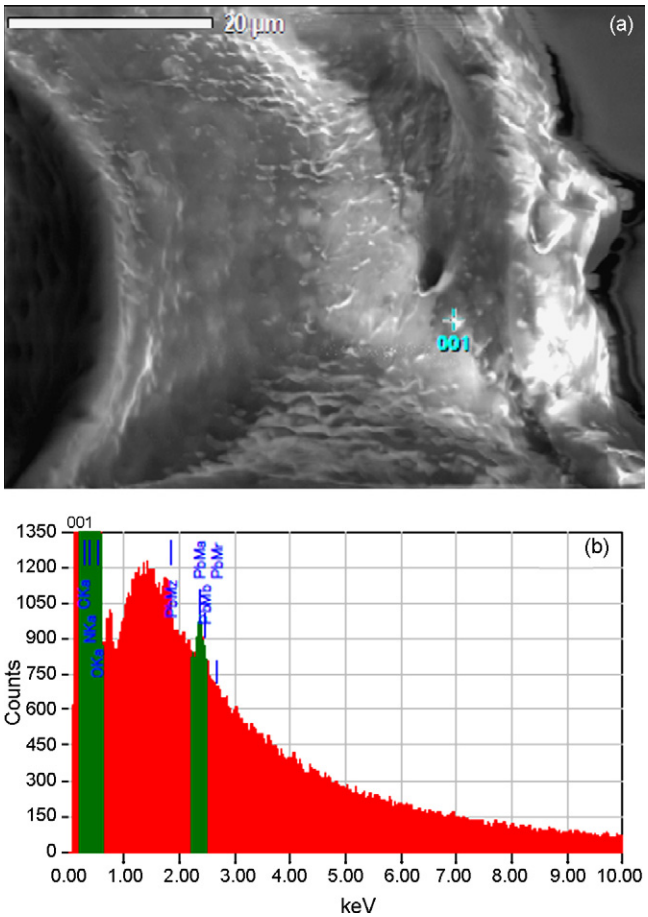


**Fig. 5.** Analysis of the adsorbed Pb using SEM-EDS. (a) SEM image of the surface of $Pb^{2+}$–ALG/PUCF sample and (b) the location used for EDS analysis denoted as 001. SEM-EDS conditions were 2.4 keV at accelerating voltage of 20.0 kV; irradiation current of 1.0 nA.

of the alginate. In other words, alginate in the acidic form, namely the alginic acid, was less sensitive to $Pb^{2+}$ ions.

### 3.4. Effect of alginate percentage in ALG/PUCF on adsorption capacity

The mixing ratio for NB-9000B, precursor ALG solution, and Pluronic L-62 was set at 100/100/1 (w/w/w). To test the effect of

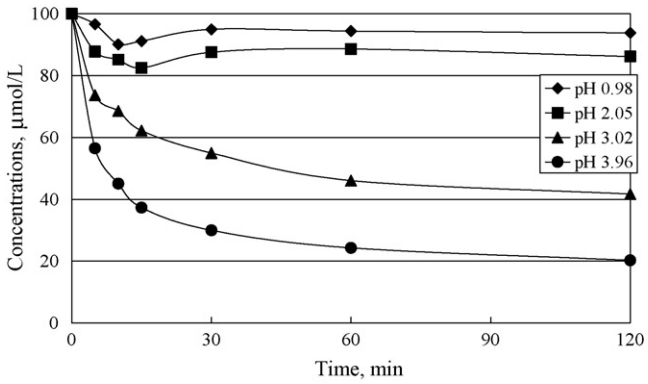


**Fig. 6.** Effect of pH of the sample solution on the adsorption of $Pb^{2+}$ ions by the ALG/PUCF. Initial concentration of $Pb^{2+}$ ions in all samples was 100.0 μM. Each sample volume was 100.0 ml. The measured ALG/PUCF of dry weights were 0.502, 0.501, 0.502, and 0.503 g, respectively.

ALG concentration, the weight percentage of alginate in the precursor ALG solution was varied from 0.2% to 3.0% and the resultant ALG/PUCF was used as the adsorbent. The capacity of the ALG/PUCF to adsorb $Pb^{2+}$ ions increased with increasing percentage of alginate in the precursor solution. However, ALG/PUCF with the desired open cells could not be obtained for the precursor ALG solutions of higher concentration (2.0% and 3.0%). ALG/PUCF obtained using 1.0% ALG as the precursor ALG solution was used as the typical (optimized) adsorbent for further adsorptive studies. This version of ALG/PUCF was found to contain $38.2 \pm 1.2$ μmol (average of five measurements) of carboxyl groups ($COO^-$) for 1.0 g of ALG/PUCF of dry weight.

### 3.5. Sorption isotherm

Adsorption of $Pb^{2+}$ ions by ALG/PUCF for samples containing different initial concentrations of the metal ion was carried out; for all sample solutions in this experiment, the pH was adjusted to pH 4.02. The data for plotting the adsorption curve were obtained under identical (room) temperature; the adsorption curve is therefore an isotherm. As $Pb^{2+}$ ions are absorbed onto the ALG/PUCF, the adsorption rate decreases and the rate of $Pb^{2+}$ desorption increases. When the rates of adsorption and desorption are equal, adsorption/desorption equilibrium has been reached. The adsorption data can be fit to the following equation, called the linearized Langmuir equation:

$$\frac{C_A}{q_A} = \frac{C_A}{Q} + \frac{1}{QK_A} \quad (1)$$

which was derived from the following Langmuir equation:

$$q_A = \frac{QK_AC_A}{1 + K_AC_A} \quad (2)$$

where $q_A$ represents the amount of metal ions of a certain species captured per unit weight of the ALG/PUCF (μmol/g) at the final equilibrium concentration. $K_A$ is the Langmuir constant relating to the affinity of the binding sites and is considered as a measure of the adsorption energy. $C_A$ is the equilibrium concentration (μmol/l) in solution and $Q$ is the maximum adsorption capacity at monolayer (μmol/g). Fig. 7 shows the plots of adsorption isotherm, namely the amount of $Pb^{2+}$ adsorbed by ALG/PUCF *versus* the concentration of $Pb^{2+}$ in the sample solutions at the adsorption/desorption equiliriums. Adsorption isotherms for $Cd^{2+}$, $Co^{2+}$, $Mn^{2+}$, $Mg^{2+}$ and $Ca^{2+}$ obtained under identical experimental conditions were also given in Fig. 7, for comparison. $Q$ and $K_A$ were calculated; Table 1 summarizes resultant data. As can be seen from Table 1, the adsorption of these metal ions by ALG/PUCF fitted well ($R$ was in the range of 0.982–1.000) with the Langmuir equation under the concentration range evaluated in this study, suggesting the presence of a finite number of homogenous binding sites (the carboxyl groups) on the ALG/PUCF. The $K_A$ for $Pb^{2+}$ was 11.01; for $Cd^{2+}$, $Ca^{2+}$, $Co^{2+}$, $Mn^{2+}$ and $Mg^{2+}$ it was 8.41, 7.63, 4.99, 3.09, and 1.15, respectively. In other words, $Pb^{2+}$ ions show the highest affinity toward the ALG/PUCF, followed by $Cd^{2+}$, $Ca^{2+}$, $Co^{2+}$, $Mn^{2+}$ and $Mg^{2+}$.

**Table 1**
Parameters of the Langmuir isotherm plots for six divalent cation species

| | $Ca^{2+}$ | $Cd^{2+}$ | $Co^{2+}$ | $Mg^{2+}$ | $Mn^{2+}$ | $Pb^{2+}$ |
|---|---|---|---|---|---|---|
| $Q$ (μmol/g) | 17.06 | 14.66 | 15.53 | 8.84 | 16.18 | 15.95 |
| $K_A$ | 7.63 | 8.41 | 4.99 | 1.15 | 3.09 | 11.01 |
| $R^2$ | 0.9817 | 0.9996 | 0.9912 | 0.9977 | 0.9989 | 0.9867 |

Other experimental conditions were the same as described in Fig. 4.

### 3.6. Adsorption of $Pb^{2+}$ ions in samples containing competitive ions

Aqueous solutions containing $Pb^{2+}$ ions along with other competing metal ions were prepared. These solutions were then used to study the selectivity for adsorbing $Pb^{2+}$ ions in the presence of other metal ion species. A series of aqueous solutions was prepared, each containing $Cd^{2+}$, $Mg^{2+}$, and $Ca^{2+}$ (100.0 μM of each ion) and $Pb^{2+}$ varying from 0 to 100.0 μM. Those solutions were then tested with the ALG/PUCF adsorbent. Fig. 8 shows the resulting data plotted as the molar quantity of the metal ions being adsorbed by ALG/PUCF *versus* the initial concentration of $Pb^{2+}$ ions in the aqueous solution. As can be seen from Fig. 8, the amount of the $Pb^{2+}$ adsorbed onto ALG/PUCF was found to increase proportionally with the increase of initial $Pb^{2+}$ concentration in the solution. For $Cd^{2+}$ and $Ca^{2+}$, on the other hand, the adsorbed molar amount decreased almost linearly as the initial concentration of $Pb^{2+}$ in the samples increased. $Mg^{2+}$ ions were adsorbed in very small quantities for all lead concentrations tested. These results again indicate that, among the metal ions tested, the ALG/PUCF has the highest affinity for adsorbing $Pb^{2+}$, followed by $Cd^{2+}$, $Ca^{2+}$, and $Mg^{2+}$. The maximum $Pb^{2+}$ adsorption capacity for the optimized ALG/PUCF sample containing an overall $19.1 \pm 1.2$ μmol of carboxyl groups (the binding site) was found to be $9.1 \pm 2.1$ μmol. In other words, at the maximum capacity, the ratio of carboxyl groups to $Pb^{2+}$ ions captured in the ALG/PUCF was approximately 2:1 (mol/mol).

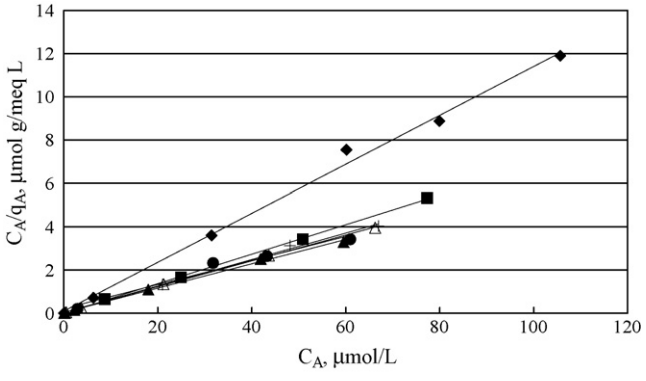


**Fig. 7.** Langmuir plots for adsorption of $Pb^{2+}$ (■), $Cd^{2+}$ (▲), $Co^{2+}$ (△), $Mn^{2+}$ (+), $Mg^{2+}$ (♦) and $Ca^{2+}$ (●) ions by ALG/PUCF.

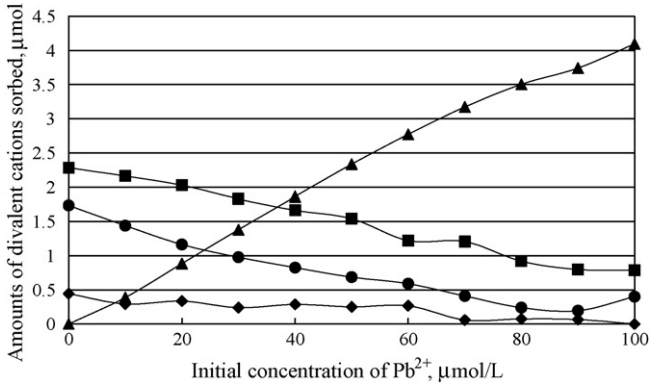


**Fig. 8.** Adsorption of $Pb^{2+}$ ions (▲) in the presence of competing ions in the sample solutions. The competing ions in the samples were $Mg^{2+}$ (♦), $Ca^{2+}$ (●), and $Cd^{2+}$ (■), each at a concentration of 100.0 μM. The $Pb^{2+}$ concentration was varied from 0 to 100.0 μM in these samples. The pH of all samples was 4.02. Sample volume, 50.0 ml; ALG/PUCF, 0.25 g of the dry weight.

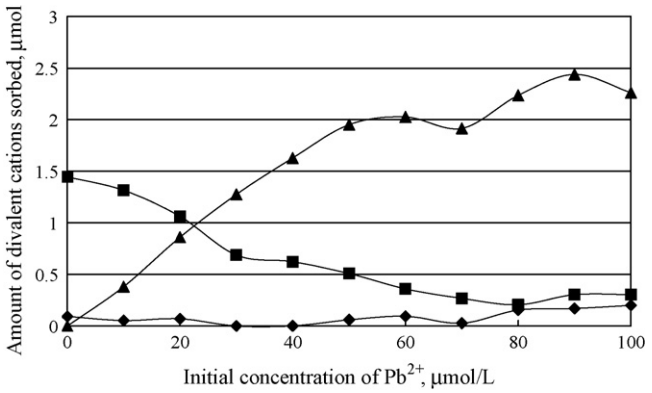


**Fig. 9.** Adsorption of $Pb^{2+}$ ions (▲) in the presence of competing ions in the sample solutions using alginate–$Ca^{2+}$ beads as the adsorbents. The two competing ions in these samples were $Mg^{2+}$ (♦) and $Cd^{2+}$ (■), each at a concentration of 100.0 μM. The $Pb^{2+}$ concentration was varied from 0 to 100.0 μM in these samples. The pH of all samples was 4.02. Total amounts of carboxyl groups are same as Fig.8.

### 3.7. Adsorption using alginate/calcium(II) hydrogel adsorbents

Alginate was immobilized using a traditional method of hydrogel formation using calcium ions ($Ca^{2+}$) as the cross-linking ions. Fig. 9 shows the adsorptive experimental data obtained by using the ALG–$Ca^{2+}$ hydrogel beads with average diameters of 300 μm as the adsorbents. Aqueous solutions were prepared containing ions each at a constant concentration of 100.0 μM, while varying the concentration for $Pb^{2+}$ ions from 0 to 100.0 μM, as in the experiments described in Fig. 8. In the concentration range of 0–50.0 μM, the number of $Pb^{2+}$ ions adsorbed by the ALG–$Ca^{2+}$ beads increases almost linearly with the increase of initial $Pb^{2+}$ concentration in the samples. After the initial $Pb^{2+}$ concentration exceeds 60.0 μM, however, the adsorptive capacity for $Pb^{2+}$ ions remained almost unchanged. As with the ALG/PUCF, the ALG–$Ca^{2+}$ beads showed higher selectivity for adsorbing $Pb^{2+}$ than for $Mg^{2+}$ or $Cd^{2+}$.

Fig. 10 shows the sorption isotherms plotted using the data from the hydrogel experiments. For $Mg^{2+}$ and $Cd^{2+}$, the experimental data fit well with the Langmuir adsorption model, suggesting that these two species were adsorbed via a monolayer adsorption process. However, for $Pb^{2+}$, the Langmuir adsorption model was not applicable, indicating a unique mechanism of adsorption for $Pb^{2+}$ ions by the ALG–$Ca^{2+}$ beads. The maximum capacity for the ALG–$Ca^{2+}$ beads containing overall 144.1 ± 1.2 μmol (average of three measurements) of carboxyl groups was found to be 24.2 ± 2.1 μmol (average of three measurements) for adsorption of $Pb^{2+}$ ions. In other words, at maximum capacity, the ratio of carboxyl groups in the alginate–$Ca^{2+}$ beads to $Pb^{2+}$ ions captured was approximately 6:1 (mol/mol). This ratio was significantly lower for ALG/PUCF, indicating more efficient capture of $Pb^{2+}$ ions by ALG/PUCF compared to the hydrogel adsorbent.

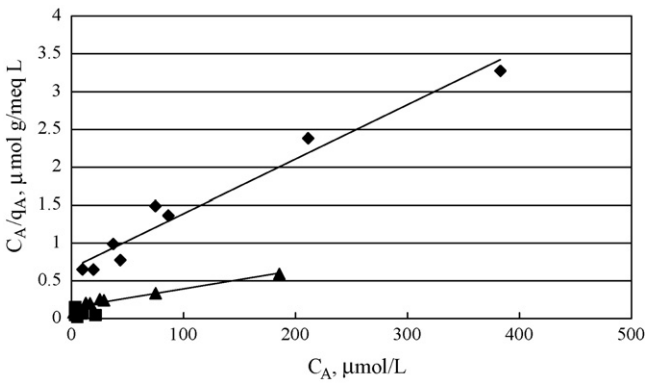


**Fig. 10.** Langmuir plots for adsorption of $Mg^{2+}$ (♦), $Cd^{2+}$ (▲) and $Pb^{2+}$ (■) using alginate–$Ca^{2+}$ beads as the adsorbents.

### 3.8. Mechanism of adsorption of $Pb^{2+}$ ions by ALG/PUCF

Compared to the conventional ALG–$Ca^{2+}$ beads, ALG/PUCF shows a unique behavior for the adsorption of $Pb^{2+}$ ions. Unlike ALG–$Ca^{2+}$, the alginate in ALG/PUCF was immobilized chemically by binding its sugar backbone to the NB-9000B prepolymer. Our explanation of the mechanism of $Pb^{2+}$ binding by the ALG/PUCF is therefore summarized in terms of an electrostatic interaction model, namely the ion-exchange model. The essential concepts of this model are summarized as follows:

(1) In ALG/PUCF, alginate was immobilized by chemical reactions between the hydroxyl groups of the alginate sugar backbone and the isocyanate groups of the NB-9000B prepolymer. The FT-IR data support this conclusion. In the ALG–$Ca^{2+}$ beads, on the other hand, alginate was immobilized during the hydrogel formation by specific binding of $Ca^{2+}$ ions to the polysaccharide, leading to a firm cohesion between the polyelectrolyte chains [22].
(2) In ALG/PUCF, all the carboxyl groups can function as the binding sites for capturing $Pb^{2+}$ ions. The molar ratio of the available carboxyl groups to the captured $Pb^{2+}$ was found to be 2:1; this gives evidence to support this conclusion. In contrast, in the alginate–$Ca^{2+}$ beads, the molar ratio of the available carboxyl groups to the captured $Pb^{2+}$ was 6:1, indicating some of the carboxyl groups have no ability for binding $Pb^{2+}$. They were spent on interaction with $Ca^{2+}$ ions in formation of the $Ca^{2+}$–alginate hydrogel [23].
(3) In ALG/PUCF, $Pb^{2+}$ ions were retained mainly by electrostatic interaction by replacement of sodium ions ($Na^{+}$) from the carboxyl groups on alginate. In other words, ALG/PUCF behaved as an ion-exchanger with carboxyl groups as the functioning sites. The fact that the sorption isotherm for $Pb^{2+}$ ions fitted well with the Langmuir adsorption model supports this conclusion. On the other hand, in the alginate–$Ca^{2+}$ beads, cations having smaller affinity than $Ca^{2+}$ (the cross-linking ions), such as $Mg^{2+}$ and $Cd^{2+}$ ions, were also retained based on ion-exchange of $Na^{+}$ ions from the carboxyl groups on alginate and therefore undergoing the monolayer adsorption (fitting well with the Langmuir adsorption model). However, for the $Pb^{2+}$ ions, their affinity toward alginate was higher than that for $Ca^{2+}$, the cross-linking ions. As a result, a more firmed type of hydrogels was formed by formation of the $Pb^{2+}$–alginate complexes. The sorption isotherm for $Pb^{2+}$ did not fit the Langmuir sorption model, indicating the adsorption of $Pb^{2+}$ ions are undergoing a much complicated manner by the $Ca^{2+}$–alginate beads.

### 3.9. Regeneration of the $Pb^{2+}$–ALG/PUCF using EDTA-2Na

The ALG/PUCF was reusable by using aqueous EDTA-2Na solution as the regeneration solution. The adsorbed $Pb^{2+}$ ions were converted into $Pb^{2+}$–EDTA, which is an anionic complex showing no affinity toward ALG/PUCF. After four cycles of adsorption and regeneration, the capacity for adsorbing $Pb^{2+}$ ions was found to be almost identical to the initial capacity, demonstrating the high reusability of the ALG/PUCF.

## 4. Conclusion

We have shown that hydrophilic, flexible polyurethane foams containing alginate are capable of selectively adsorbing $Pb^{2+}$ ions. Alginate was immobilized chemically in the cell walls of the polyurethane foam. The carboxyl groups on the alginate are the functional sites for capturing $Pb^{2+}$ ions. The ALG/PUCF shows a higher affinity for $Pb^{2+}$ than for other metal ions due to the nature of the poly-carboxylic ion-exchanger. The sodiumalginate/polyurethane composite foam is robust, mechanically strong, durable, and easy to produce. Its high surface area and high reusability provide a practical and simple approach for the selective elimination of $Pb^{2+}$ from contaminated water. Use of the ALG/PUCF adsorbent for elimination of $Pb^{2+}$ from contaminated soil is under investigation by our research group.

## References


[1] D. Quig, Cysteine metabolism and metal toxicity, Altern. Med. Rev. 3 (1998) 262–270.
[2] G. Kiley, Environmental Engineering, McGraw-Hill, New York, 1997.
[3] M. Markowitz, Lead poisoning, Pediatr. Rev. 10 (2000) 327–335.
[4] P.M. Kopittke, C.J. Asher, R.A. Kopittke, N.W. Menzies, Toxic effects of $Pb^{2+}$ on growth of cowpea (*Vigna unguiculata*), Environ. Pollut. 150 (2007) 280–286.
[5] J.B. Christensen, J.J. Botma, T.H. Christensen, Complexation of Cu and Pb by DOC in polluted groundwater: a comparison of experimental data and predictions by computer speciation models (WHAM and MINTEQA2), Water Res. 33 (1999) 3231–3238.
[6] A.L. Nolan, H.M.J. Mclaughlin, S.D. Mason, Chemical speciation of Zn, Cd, Cu and Pb in pore waters of agricultural and contaminated soils using Donnan dialysis, Envrion. Sci. Technol. 37 (2003) 90–98.
[7] D. Petruzzelli, M. Pagano, G. Tiravanti, R. Passino, Lead removal and recovery from battery wastewaters by natural zeolite clinoptilolite, Solvent Extract. Ion Exchange 17 (1999) 677–694.
[8] M.M. Husein, J.H. Vera, M.E. weber, Removal of lead from aqueous solutions with sodium caprate, Sep. Sci. Technol. 33 (12) (1998) 1889–1904.
[9] S.W. Lin, R.M.F. Navarro, An innovative method for removing $Hg^{2+}$ and $Pb^{2+}$ in ppm concentrations from aqueous media, Chemosphere 39 (11) (1999) 1809–1817.
[10] T. Mohammadi, A. Razmi, M. Sadrzadeh, Effect of operating parameters on $Pb^{2+}$ separation from wastewater using electrodialysis, Desalination 167 (2004) 379–385.
[11] K. Perisamy, C. Namasivam, Removal of copper(II) by adsorption onto peanut hull carbon from water and lead plating industry wastewater, Chemosphere 32 (1996) 769–789.
[12] N. Kannan, J. Balamurugan, Removal of lead ions by adsorption onto coconut shell and dates nut carbons, a comparative study, Indian J. Environ. Protect. 25 (9) (2005) 816–823.
[13] C.K. Singh, J.N. Sahu, K.K. Mahalik, C.R. Mohanty, B. Raj Mohan, B.C. Meikap, Studies on the removal of Pb(II) from wastewater by activated carbon developed from Tamarind wood activated with sulphuric acid, J. Hazard. Mater. 153 (2008) 221–228.
[14] M. Kazemipour, M. Ansari, S. Tajrobehka, M. Majdzadeh, H.R. Kermani, Removal of lead, cadmium, zinc and copper from industrial wastewater by carbon developed from walnut, hazelnut, almond, pistachio shell and apricot stone, J. Hazard. Mater. 150 (2008) 322–327.
[15] B.M. Amarasinghe, R.A. Williams, Tea waste as a low cost adsorbent for the removal of Cu and Pb from wastewater, Chem. Eng. J. 132 (2007) 299–309.
[16] S.F. Montanher, E.A. Oliveira, M.C. Rollemberg, Removal of metal ions from aqueous solutions by sorption onto rice bran, J. Hazard. Mater. B117 (2005) 207–211.
[17] S.S. Ahluwalia, D. Goyal, Removal of heavy metals by waste tea leaves from aqueous solution, Eng. Life Sci. 5 (2) (2005) 158–162.
[18] M.M.D. Zulkali, A.L. Ahmad, N.H. Norulakmal, *Oryza sativa* L. husk as heavy metal adsorbent: optimization with lead as model solution, Bioresour. Technol. 97 (2006) 21–25.
[19] S.K. Papageorgiou, F.K. Katsaros, E.P. Kouvelos, J.W. Nolan, H.L. Deit, N.K. Kanellopoulos, Heavy metal sorption by calcium alginate beads from *Laminaria digitata*, J. Hazard. Mater. B137 (2006) 1765–1772.
[20] L. Zgang, J. Zhou, D. Zhou, Y. Tang, Adsorption of cadmium and strontium on cellulose/alginic acid ion-exchange membrane, J. Membr. Sci. 162 (1999) 103–109.
[21] B. Fugetsu, S. Satoh, T. Shiba, T. Mizutani, Y. Lin, N. Terui, et al., Caged multiwalled carbon nanotubes as the adsorbents for affinity-based elimination of ionic dyes, Environ. Sci. Technol. 38 (2004) 6890–6896.
[22] G.T. Grant, E.R. Morris, D.A. Rees, P.J.C. Smith, D. Thom, Biological interactions between polysaccharides and divalent cations: the egg-box model, FEBS Lett. 32 (1973) 195–198.
[23] J.P. Ibáñez, Y. Umetsu, potential of proponated alginate beads for heavy metal uptake, Hydrometallurgy 64 (2002) 89–99.